

Document downloaded from:

<http://hdl.handle.net/10251/193142>

This paper must be cited as:

Barrientos, K.; Rocha Gaso, Ml.; Jaramillo, M.; Aldrín Vásquez, N. (2022). High Frequency (100, 150 MHz) Quartz Crystal Microbalance (QCM) Piezoelectric Genosensor for the Determination of the Escherichia coli O157 rfbE Gene. *Analytical Letters*. 55(17):2697-2709. <https://doi.org/10.1080/00032719.2022.2068566>







The final publication is available at

<https://doi.org/10.1080/00032719.2022.2068566>

Copyright Taylor & Francis

Additional Information

High frequency (100, 150 MHz) quartz crystal microbalance (QCM) piezoelectric genosensor for the determination of the *Escherichia coli* O157 *rfbE* gene

Kaory Barrientos^{1,*}, María Isabel Rocha², Marisol Jaramillo¹, Neil Aldrin Vásquez³

¹ *GIBEC Research Group, Life Sciences Faculty, Universidad EIA, Calle 25 Sur #42-73 055420, Medellín, Colombia*

² *Advanced Wave Sensors S. L., Calle Algepser 24 46988, Valencia, Spain*

³ *BioA Research Group, Biosciences Faculty, Universidad Nacional de Colombia, Carrera 65 #59A-110 050034, Medellín, Colombia*

**Corresponding author: kaory.barrientos@eia.edu.co; (+57) 604 354 9090*

High frequency (100, 150 MHz) quartz crystal microbalance (QCM) piezoelectric genosensor for the determination of the *Escherichia coli* O157 *rfbE* gene

Escherichia coli O157 (*E. coli* O157) is responsible for outbreaks of high morbidity in food-borne infections. The development of sensitive, reliable, and selective detection systems is of great importance in food safety. In this work, it was designed and validated two high fundamental frequency (HFF) piezoelectric genosensor (100 and 150 MHz) for the *rfbE* gene detection, which encodes O-antigen in *E. coli* O157. HFF resonators offer improved sensitivity, small sample volumes, and the possibility of integration into lab-on-a-chip devices, but their sensing capabilities have not yet been fully explored. This HFF-QCM genosensor uses the method of physisorption based on the union between the streptavidin protein and the biotin molecule to immobilize the genetic bioreceptor on the surface and detect its hybridization with the target sequence. Parameters such as molecular coating, specificity, and variability have been tested to enhance its performance. Although, the genosensors evaluated can determine the target, the 100 MHz device has a higher response to the analyte than the 150 MHz platform. This is the first step in the development of an HFF-QCM genosensor that could be used as a trial test of *E. coli* O157 in large batch samples.

Keywords: genosensor; quartz crystal microbalance piezoelectric; high frequency; *E. coli* O157

Introduction

Biosensors are devices that couple biological interfaces to a transduction system that transforms a biological recognition event between the analyte of interest and its specific receptor into a signal that can be measured and quantified (Pohanka 2018). The genosensors are biosensors for detecting genomic material based on the nucleic acid hybridization events as the underlying molecular recognition interaction (Ortiz et al. 2020).

Genosensors based on Quartz Crystal Microbalance with Dissipation (QCMD) detect nucleic acid hybridization events through changes in the resonance frequency and dissipation of the piezoelectric resonators (Miloni et al. 2020). They are inherently label-free.

Conventional QCMD-based biosensors use resonance frequencies between 5 and 30 MHz. It is expected that the use of resonators with high fundamental frequencies (HFF resonators) would improve the sensitivity and reduce reagent consumption (Polshettiwar et al. 2021). The improvement in sensitivity arises from the relationship between the fundamental resonance frequency and frequency shift due to a given mass, $\Delta f = -2.269 \times 10^{-15} f^2 \Delta m$ (Sauerbrey 1959). Since the resonator's resonance frequency is inversely proportional to its thickness, HFF resonators are much thinner than their classical low-frequency counterparts. Resonator design constraints dictate that thinner resonators must also be smaller in the lateral dimensions (Bottom 1982). Indeed, the 100 and 150 MHz resonators used in this study have sensing areas of 0.4 mm² and can work with volumes as low as 4 μ l, compared with \sim 1 cm² and 40 μ l for a typical 5 MHz sensor (Fernández et al. 2017).

The promise of improved sensitivity and reduced sample volume make HFF-QCMD resonators interesting tools for genosensor development. However, until now, HFF-QCMD biosensors have been used for developing immunoassays (March et al. 2015; Montoya et al. 2017; Cervera-Chiner et al. 2018; Buitrago et al. 2020), where, indeed, an improvement in sensitivity has been demonstrated (March et al. 2015). Therefore, the development of this work focused on the development of an HFF-QCMD genosensor.

As a model system, a sequence of the *rfbE* gene was detected, which encodes the O157 antigen in *E. coli* (Wang and Reeves 1998; Zhou et al. 2020). The O157

strains are the most isolated Shiga toxin (Stx)-producing *E. coli* (STEC) strains worldwide (Schmidt et al. 1999), and they are of great importance in public health. The Center for Disease Control and Prevention (CDC) of the United States estimates that 265,000 infections caused by *E. coli* are detected each year, of which 36 % are due to the action of the *E. coli* O157 strain (Centers for Disease Control and Prevention 2019). Although the reported outbreaks in the US for this strain have decreased since 1999, sporadic cases continue to occur, so the burden on the government has been estimated at \$405 million, including losses in productivity, medical care, and premature death (Lim et al. 2010; Heiman et al. 2015). In this work, they immobilized the oligonucleotide probes for the *rfbE* gene on the resonator surface via streptavidin-biotin interaction and used it to detect probe DNA comprising a part of the *rfbE* gene. The performance of the genosensor, based on resonators, was evaluated with two frequencies (100 MHz and 150 MHz) by assessing their specificity and variability.

Materials and methods

Reagents

The reagents used for the functionalization of the quartz crystals with a gold electrode were from Merck[®], including phosphate-buffered saline (PBS) 0.1 M pH 7.5, sodium dodecyl sulfate 20 % (SDS), potassium hydroxide (KOH), 50 % hydrogen peroxide (H₂O₂), ultrapure ethanol (CH₃CH₂OH), streptavidin and biotin (C₁₀H₁₆N₂O₃S). Cobas Cleaner[®] is exclusively produced and distributed by Hoffman-La Roche[®], and the oligonucleotides with their respective modifications were from the company Eurogentec[®] (Table 1).

HFF-QCM methodology

In the experiments, commercially available, gold-coated AT-cut quartz HFF resonators with the fundamental frequencies of 50 MHz and 100 MHz from Awsensors S.L. (Valencia, Spain; www.awsensors.com) were used. The experiments of the 100 MHz crystal were at its fundamental frequency and the 50 MHz HFF-QCM were in the third harmonic of the fundamental frequency (150 MHz). They were mounted in the Quick-Lock HFF flow cells (Awsensors) and installed in the A20+ platform (Awsensors) for characterizing the response of the resonators in real-time [4]. The flow cells were connected to the F20 fluidics platform (Awsensors) equipped with a Degasi[®] Compact degasser (Biotech, Onsala, Sweden) for flowing the buffer and injecting the samples over the surfaces of the resonators. The software to control both the A20 and the F20 was the Awsuite software (Awsensors), which recorded the data (frequency, dissipation, and volume of solution flowing) as a function of time. Data was exported to extract frequency shifts and converted to mass changes using the Sauerbrey relationship (1) (Sauerbrey 1959).

$$\Delta f = -\frac{2Nf^2}{A_p\sqrt{\mu_p\rho_p}}\Delta m \quad (1)$$

Where Δm is the mass deposited on the sensitive area and causes a change in the resonator frequency (Δf), A_p is the sensitive area (0.4 mm²), μ_p the shear modulus of quartz for AT-cut crystal, ρ_p the density of the resonator (quartz), f is the natural frequency resonance, and N is the harmonic.

The cleaning of the fluidics of the F20 was using an established cleaning protocol using a sequence of cobas, ethanol, and water as cleaning reagents (AWSensors 2019).

Sensor functionalization and hybridization protocol

Figure 1 shows the surface functionalization, performed in situ, using the streptavidin – biotin-binding methodology. The crystals were cleaned for 30 min with 2 % SDS solution, rinsed with water, and dried with nitrogen gas. Then, the crystals were treated, for 30 min, with UV/Ozone Procleaner™ Plus (Bioforce nanosciences, USA) previously pre-heated for 30 min. The gold-coated quartz crystals were mounted in the flow cells, then installed on the A20 platform, and connected to the F20 fluidics platform. 0.1 M PBS pH 7.5 buffer was allowed to flow through the cells, and frequency and dissipation data were collected as a function of time until a stable baseline signal.

50 µg/mL streptavidin solution in buffer was injected to establish a functionalized surface, followed by 1 µM of the DNA-c probe (bioreceptor). Finally, 100 µM of biotin was used to block undesired interactions on the remaining sites on the streptavidin.

For the hybridization process, 300 µL of the DNA-t (target) was passed over the surface of the sensor modified with the cDNA probe at various concentrations. Detection of the DNA hybridization was performed by injecting, 50 µg/mL streptavidin solution.

All tests were carried out at room temperature (25 °C) and constant flow rate (50 µL/min). Oligonucleotides were previously heated for 3 min at 95 °C, before being introduced into the F20 and A20+ platforms. Figure 2 shows the tests performed on the crystals.

The experimentally measured dissipation values suggest that the frequency shifts could be interpreted in terms of the adsorbed mass using the Sauerbrey equation (1) (Sauerbrey 1959). Unusually, the dissipation changes due to the adsorption of

streptavidin used in the immobilization process were negative. We attribute this behavior to the changes in the surface roughness associated with the streptavidin adsorption onto gold and show that it does not affect the subsequent analysis. The quantification of the substrate's surface mass adsorbed for streptavidin is included in the analysis of this work.

Results and discussion

Immobilization and hybridization of DNA probes on 50 MHz crystals

The first step in the experimental approach is to inject streptavidin solution. The corresponding adsorption step labeled {1} is visible in Figure 3. On average, streptavidin yielded a frequency shift of -2922 ± 219 Hz (the average of 6 experiments), corresponding to the mass of 474 ± 75 ng/cm², close to the mass of streptavidin reported in the classical studies by Höök *et al.* (Höök *et al.* 2001), with a value of ~ 470 ng/cm².

In the fourth step, the biotin solution passed through the fluidic system, and a change in the frequency variation is not observed because the molecular weight of biotin is 244 Da (Karlsson and Ståhlberg 1995), which is too small to be detected with the QCM.

To verify the hybridization process, in the sixth step, added streptavidin, is expected to interact with the biotin that is exposed on the DNA-t probe, in case the DNA-t has interacted with the surface-immobilized DNA-c (if DNA-c and DNA-t are complementary). This step is necessary to amplify the DNA hybridization signal, which can be too small to detect with the QCM if the DNA concentration in the sample is lower, and this step represents the interaction between streptavidin and the complementary chain conjugated biotin. This strategy could corroborate the hybridization phenomenon, since, in case the DNA double chain is not formed, the

DNA-t could link to the gold surface by two mechanisms: i) if not been correctly blocked, it could immobilize through the biotin-conjugated at its 5' end to the streptavidin fixed on the surface (Rashid and Yusof 2017); ii) the DNA-t could interact with the gold surface through the amines available in its bases, in this case, the DNA could have a conformation parallel to the crystal surface (Carrascosa et al. 2009). Even if these cases occurred, the biotin molecules present in the DNA-t would not be accessible to the streptavidin of the last injection, so there would be no variations in the vibrational frequency of the crystal. However, as shown in the sixth step, the injection of the streptavidin solution produces a change in frequency, which has to do with the fact that the hybridization phenomenon occurred successfully.

Given that the frequency variation when injecting the DNA-c (steps labeled {2} and {3}) was $255 \pm 73 \text{ ng/cm}^2$ (Table 2), its molecular weight is 14568 g/mol, and the mass of streptavidin obtained in the previous step {1} was $479 \pm 63 \text{ ng/cm}^2$; the number of molecules of DNA-c which could interact with streptavidin is between 1.8 and 2.8. However, according to the assembly of streptavidin on the gold surface, the protein has two available sites of interaction with biotin (Dubacheva et al. 2017), so the surplus DNA molecules with biotin probably interacted through the amines with the gold surface.

The change in injecting the DNA-t (fifth step) was $115 \pm 32 \text{ ng/cm}^2$, and the molecular weight of DNA-t is 9382.3 g/mol, so the number of DNA-t molecules that hybridize with the DNA-c is between 0.6 and 1, suggesting that the remaining bioreceptor molecules were inaccessible to the target. The difference between DNA-c and DNA-t can be given by the intrinsic defects associated with the crystal surface, such as roughness, the separation between gold atoms, and cracks. This causes a non-uniform immobilization of the protein on the surface and, therefore, the cession of free space on

the gold to interact with the amines of the DNA bases through a donation/donation mechanism (Hoft et al. 2007; De La Llave et al. 2014). Likewise, different authors, such as Dolatshahi-Pirouz *et al.* (Dolatshahi-Pirouz et al. 2008) and Rechendorff *et al.* (Rechendorff et al. 2006), studied the direct adsorption of proteins on platinum and tantalum surfaces, respectively. In their investigations, they found that the surface density of the protein increased with the roughness value of the substrate, which is, while more nano heights above the reference plane exist, it will be greater the mass of protein molecules deposited on a unit area because the surface area probably increased. These results suggest that, although the roughness of the crystal surface favors non-specific adsorption on the substrate, it also increases the surface area and, therefore, favors interaction with other molecules such as DNA-c. This duality in the intrinsic properties of the substrate manufacturing process could explain the increase in the number of DNA-c probes immobilized in the model since it considers a flat surface and free of defects, and why not all DNA-t molecules hybridize.

On the other hand, the variation when injecting streptavidin after the hybridization process was $241 \pm 50 \text{ ng/cm}^2$, indicating that 73.3 % of the DNA-t bound to at least one active site of the protein. While the remaining 26.7 % probably did not interact because the excess of biotin groups in densely molecular layers imposes steric constraints that limit the binding of biotin with the interaction sites of streptavidin (Rusmini et al. 2007; Wolny et al. 2009; Sandhyarani 2019).

Molecular coating

Because the hybridization process depends on obtaining an organized, dense, and structured surface, the number of injections necessary to form a DNA layer with a high molecular coating has been studied.

The interest of this study is in achieving high molecular coverage, for which it has been determined that the parameter that allows identifying the proportion of surface molecules that are interacting between them is the change in the frequency variable. The substrate saturates when a variation of less than 100 Hz was obtained since this value represents the average signal noise, so a change of this magnitude implies variations associated with the operation of the device. According to the data obtained (Table 3 and Figure S1), it is only necessary to perform two injections of the DNA-c. Probably because by injecting the streptavidin protein that interacts with gold, a high molecular coating is achieved. Therefore, the DNA probe influx does not have enough time to bind with all available sites on the surface of the crystal. The first injection of the DNA-c produced a mass change of 218 ng/cm², equivalent to 7.12x10¹⁰ molecules. According to the molecular model proposed for the immobilization process, this value indicates that 80 % of the active sites of streptavidin immobilized on the surface interact with the DNA bioreceptor molecules. However, by performing the second injection, not only is 100 % interaction achieved but 6 % more molecules are immobilized likely through non-specific interactions with the gold surface.

On the other hand, the second injection of the DNA-t produces a change of less than 100 Hz and a positive change in the variation of the frequency (22.5 Hz), which is equivalent to a negative change in mass of -4.04 ng/cm². This implies that there was probably desorption of molecules caused by the interaction between DNA-c immobilized by non-specific interactions on the gold surface and DNA-t molecules.

Variability

The standard deviation (SD) analysis was implemented through a descriptive observational cross-sectional study to determine the variability between DNA

hybridization assays carried out on 50 MHz crystals in the third harmonic (150 MHz). In this study, the change in mass of nine trials was recorded by injecting DNA-t. The SD gave a value of 32.7 ng/cm²; and since the detection level of the device is 33.6 ng/cm², which was determined by considering the average noise in the assays; it is suggested that the hybridization process, under the conditions analyzed in this work, has an acceptable variability; since the variation of the numerical data set is below the noise presented by the device.

Immobilization and hybridization of DNA probes on 100 MHz crystals

The measurements carried out in the fundamental mode of the piezoelectric sensors have a greater dispersion than those made in the third harmonic or higher since the vibration modes of the crystals in their respective harmonics behave as sources of energy entrapment and marginal electric fields, which translates into better signal stability. Figure 4 shows the immobilization, hybridization, and verification process on 100 MHz crystals.

The total variation of the frequency when injecting the DNA-c is 8648 Hz, which is equivalent to 361.3 ng/cm², and represents 1.17x10¹¹ DNA molecules immobilized on the surface (Table 4). According to the molecular adsorption model described for DNA hybridization, through the streptavidin-biotin binding strategy, the number of DNA-c that can specifically interact with their respective ligand is 8.96x10¹⁰, so it was possible to immobilize 31 % more DNA molecules than predicted in the model. However, by injecting the DNA-t, a change equivalent to 161 ng/cm² was obtained, equal to 8.16x10¹⁰ DNA sequences, indicating that at most 70 % of the probes immobilized on the crystal surface were hybridized and the remaining 30 % of the bioreceptor molecules were inaccessible to their respective complementary chain. This

difference corresponds to the number of molecules that probably interacted non-specifically with the gold atoms in the substrate. On the other hand, the frequency variation when injecting streptavidin protein as a strategy to verify DNA hybridization was -8529 Hz, which is equivalent to 2.8×10^{10} molecules. According to the molecular model, a streptavidin protein can interact with two biotin molecules, and, therefore, with two hybridized DNA chains. The number of protein molecules that interacted with the sensor surface indicates that 69 % of the hybridized product interacted with an active streptavidin site.

The results are consistent with the results found for the 50 MHz crystals in the third harmonic (150 MHz). However, compared to the model, the biological event of interest is more efficient on the 100 MHz sensing surface since it detects 16 % more of the hybridization process than the 50 MHz crystal, getting it closer to the molecular model proposed for this immobilization and detection strategy. Supported by the study by March *et. al* (March et al. 2015), who compared the detection efficiency between 100 MHz and 50 MHz sensors in the third harmonic and observed that the 100 MHz crystal is more sensitive than the 150 MHz crystal.

Specificity evaluation

In the fifth step (Figure S2) was injected 1 μ M of a control sequence of 26 base pairs with sequence 5'-acattaaacactaaagaacagcgttg-3', which is part of the satellite region of the nuclear DNA of the *Trypanosoma brucei* parasite. A frequency change of approximately 76 Hz was obtained (Figure S2), which is within the noise variation of the device. Therefore, it is suggested that there is no variation in the frequency of crystal vibration associated with the control sequence, indicating that the change in frequency when injecting the target occurs exclusively due to its interaction with the bioreceptor

probe.

Finally, Figure 5 shows the steps of immobilization through injections 1, 2, 3, and 4, showing binding to the surface of streptavidin, DNA-c, and the biotin molecule used to block the surface, respectively. The fifth step shows the injection of the streptavidin solution, which represents the negative control carried out during this assay. Injection 6 indicates a hybridization event, and injection 7 shows the frequency change associated with the streptavidin binding to the hybridized product. The streptavidin protein injected after the hybridization process interacts exclusively with the conjugated biotin at the 5' end of the DNA-t probe, since when injecting it before this obtained a frequency change of 296 Hz, which equals -52 ng/ m^2 . Not only implies that it did not interact with the biological interface molecules, but it produced desorption of some of the molecular structures immobilized on the surface of the piezoelectric transducer, probably because the streptavidin can interact with the conjugated biotin at the 5' end of DNA probes that are nonspecifically adsorbed on the crystal.

Conclusions

A high-frequency piezoelectric genosensor (100 and 150 MHz) was developed for the detection of the *rfbE* gene of the bacteria *E. coli* O157, through the functionalization of the transducer by a physisorption method based on the interaction between streptavidin and biotin. Under these conditions, two injections of the bioreceptor probe were necessary to obtain a more molecularly dense layer, and the 100 MHz crystal detects more efficiently the hybridization process than the 50 MHz crystals in the third harmonic (150 MHz), however, the assays at the crystal's fundamental frequency tend to be more unstable than those carried out at other vibrational modes. Furthermore, the assays carried out allowed the analysis of the specificity and variability of the developed

device, concluding that the hybridization between the bioreceptor probe and the target occurs specifically and that the tests have an acceptable variability.

Acknowledgments

The authors would like to extend their gratitude to EIA University and the National University of Colombia for the funding provided, and the company Advanced Wave Sensors S.L., for the assays carried out on their devices.

Declaration of interest statement

The authors declare no conflict of interest.

Funding details

This work was supported by the EIA University and CES University under internal call in 2016.

Data availability statement

All data generated or analyzed during this study are included in this published article and its supplementary information file.

References

- AWSensors. 2019. Cleaning Protocols :17.
- Bottom V. 1982. Introduction to Quartz Crystal Unit Design. New York: Reinhold, Van Nostrand.
- Buitrago L, Ortiz C, Barrientos K, Jaramillo M. 2020. Development of a high frequency piezoelectric immunosensor for the detection and quantification of BSA. *Biointerface Res Appl Chem.* 10(3):284–290. <https://doi.org/10.33263/BRIAC103.400405>

- Carrascosa LG, Calle A, Lechuga LM. 2009. Label-free detection of DNA mutations by SPR: Application to the early detection of inherited breast cancer. *Anal Bioanal Chem.* 393(4):1173–1182. <https://doi.org/10.1007/s00216-008-2555-1>
- Centers for Disease Control and Prevention. 2019. Timeline for reporting cases of E. coli O157 Infection; [accessed 2019 May 22]. <https://www.cdc.gov/ecoli/reporting-timeline.html>
- Cervera-Chiner L, Juan-Borrás M, March C, Arnau A, Escriche I, Montoya Á, Jiménez Y. 2018. High Fundamental Frequency Quartz Crystal Microbalance (HFF-QCM) immunosensor for pesticide detection in honey. *Food Control.* 92:1–6. <https://doi.org/10.1016/J.FOODCONT.2018.04.026>
- Dolatshahi-Pirouz A, Rechendorff K, Hovgaard MB, Foss M, Chevallier J, Besenbacher F. 2008. Bovine serum albumin adsorption on nano-rough platinum surfaces studied by QCM-D. *Colloids Surfaces B Biointerfaces.* 66(1):53–59. <https://doi.org/10.1016/j.colsurfb.2008.05.010>
- Dubacheva G V, Araya-Callis C, Geert Volbeda A, Fairhead M, Codeé J, Howarth M, Richter RP. 2017. Controlling Multivalent Binding through Surface Chemistry: Model Study on Streptavidin. *J Am Chem Soc.* 139(11):4157–4167. <https://doi.org/10.1021/jacs.7b00540>
- Fernández R, García P, García M, García J V., Jiménez Y, Arnau A. 2017. Design and validation of a 150 MHz HFFQCM sensor for bio-sensing applications. *Sensors (Switzerland).* 17(9):1–13. <https://doi.org/10.3390/s17092057>
- Heiman KE, Mody RK, Johnson SD, Griffin PM, Gould LH. 2015. Escherichia coli O157 Outbreaks in the United States, 2003-2012. *Emerg Infect Dis.* 21(8):1293–1301. <https://doi.org/10.3201/eid2108.141364>
- Hoft RC, Ford MJ, McDonagh AM, Cortie MB. 2007. Adsorption of amine compounds on the Au (111) surface: A density functional study. *J Phys Chem C.* 111(37):13886–13891. <https://doi.org/10.1021/jp072494t>
- Höök F, Ray A, Nordén B, Kasemo B. 2001. Characterization of PNA and DNA immobilization and subsequent hybridization with DNA using acoustic-shear-wave attenuation measurements. *Langmuir.* 17(26):8305–8312. <https://doi.org/10.1021/la0107704>
- Karlsson R, Ståhlberg R. 1995. Surface plasmon resonance detection and multispot sensing for direct monitoring of interactions involving low-molecular-weight

- analytes and for determination of low affinities. *Anal Biochem.* 228(2):274-280.
<https://doi.org/10.1006/abio.1995.1350>
- De La Llave E, Clarenc R, Schiffrin DJ, Williams FJ. 2014. Organization of alkane amines on a gold surface: Structure, surface dipole, and electron transfer. *J Phys Chem C.* 118(1):468–475. <https://doi.org/10.1021/jp410086b>
- Lim JY, Yoon JW, Hovde CJ. 2010. A brief overview of Escherichia coli O157:H7 and its plasmid O157. *J Microbiol Biotechnol.* 20(1):1–10.
<https://doi.org/10.4014/jmb.0908.08007>
- March C, García J V., Sánchez Á, Arnau A, Jiménez Y, García P, Manclús JJ, Montoya Á. 2015. High-frequency phase shift measurement greatly enhances the sensitivity of QCM immunosensors. *Biosens Bioelectron.* 65:1–8.
<https://doi.org/10.1016/j.bios.2014.10.001>
- March C, García J V, Sánchez A, Arnau A, Jiménez Y, García P, Manclús JJ, Montoya A. 2015. High-frequency phase shift measurement greatly enhances the sensitivity of QCM immunosensors. *Biosens Bioelectron.* 65:1–8.
<https://doi.org/10.1016/j.bios.2014.10.001>
- Milioni D, Mateos-Gil P, Papadakis G, Tsortos A, Sarlidou O, Gizeli E. 2020. Acoustic Methodology for Selecting Highly Dissipative Probes for Ultrasensitive DNA Detection. *Anal Chem.* 92(12):8186–8193.
<https://doi.org/10.1021/acs.analchem.0c00366>
- Montoya A, March C, Montagut Y, Moreno M, Manclus J, Arnau A, Jimenez Y, Jaramillo M, Marin P, Torres R. 2017. A High Fundamental Frequency (HFF)-based QCM Immunosensor for Tuberculosis Detection. *Curr Top Med Chem.* 17(14):1623–1630. <https://doi.org/10.2174/1568026617666161104105210>
- Ortiz C, Guerra JM, Jaramillo M. 2020. Immobilization of DNA probes on a high frequency piezoelectric biosensor Inmovilización de sondas de ADN en un biosensor de alta frecuencia. *DYNA.* 87(212):163–168.
<https://doi.org/10.15446/dyna.v87n212.82309>
- Pohanka M. 2018. Overview of piezoelectric biosensors, immunosensors and DNA sensors and their applications. *Mater (Basel, Switzerland).* 11(3):448.
<https://doi.org/10.3390/ma11030448>
- Polshettiwar SA, Deshmukh CD, Wani MS, Baheti AM, Bompilwar E, Choudhari S, Jambhekar D, Tagalpallewar A. 2021. Recent Trends on Biosensors in

- Healthcare and Pharmaceuticals: An Overview. *Int J Pharm Investig.* 11(2):131–136. <https://doi.org/10.5530/IJPI.2021.2.25>
- Rashid JIA, Yusof NA. 2017. The strategies of DNA immobilization and hybridization detection mechanism in the construction of electrochemical DNA sensor: A review. *Sens Bio-Sensing Res.* 16:19–31. <https://doi.org/10.1016/j.sbsr.2017.09.001>
- Rechendorff K, Hovgaard MB, Foss M, Zhdanov VP, Besenbacher F. 2006. Enhancement of protein adsorption induced by surface roughness. *Langmuir.* 22(26):10885–10888. <https://doi.org/10.1021/la0621923>
- Rusmini F, Zhong Z, Feijen J. 2007. Protein immobilization strategies for protein biochips. *Biomacromolecules.* 8(6):1775–1789. <https://doi.org/10.1021/bm061197b>
- Sandhyarani N. 2019. Surface modification methods for electrochemical biosensors. In: *Electrochem Biosens.* 1st ed.: Elsevier; p. 45–75. <https://doi.org/10.1016/B978-0-12-816491-4.00003-6>
- Sauerbrey G. 1959. Verwendung von Schwingquarzen zur Wägung dünner Schichten und zur Mikrowägung. *Zeitschrift für Phys.* 155(2):206–222. <https://doi.org/10.1007/BF01337937>
- Schmidt H, Scheef J, Huppertz HI, Frosch M, Karch H. 1999. Escherichia coli O157:H7 and O157:H– Strains That Do Not Produce Shiga Toxin: Phenotypic and Genetic Characterization of Isolates Associated with Diarrhea and Hemolytic-Uremic Syndrome. *J Clin Microbiol* 37(11):3491–3496. <https://doi.org/10.1128/jcm.37.11.3491-3496.1999>
- Wang L, Reeves PR. 1998. Organization of *Escherichia coli* O157 O antigen gene cluster and identification of its specific genes. *Infect Immun.* 66(8):3545–3551.
- Wolny PM, Spatz JP, Richter RP. 2009. On the Adsorption Behavior of Biotin-Binding Proteins on Gold and Silica. *Langmuir.* 26(2):1029–1034. <https://doi.org/10.1021/la902226b>
- Zhou W, Wang K, Hong W, Bai C, Chen L, Fu X, Huang T, Liu J. 2020. Development and Application of a Simple “Easy To Operate” Propidium Monoazide-Crossing Priming Amplification on Detection of Viable and Viable But Non-culturable Cells of O157 *Escherichia coli*. *Front Microbiol.* 11:2243. <https://doi.org/10.3389/FMICB.2020.569105/BIBTEX>

Table 1. DNA sequences.

Name	Sequence	Modification
Capture probe (DNA-c)	5' - ttt-ttt-ttt-ttt-ttt-agg-	5' Biotin – TEG
	acc-gca-gag-gaa-aga-gag- gaa-tta-agg – 3'	5' 15 thymine (Carrascosa et al. 2009)
Target probe (DNA-t)	5' - cct-taa-ttc-ctc-tct-ttc- ctc-tgc-ggt-cct– 3'	5' Biotin

Table 2. Mass and frequency changes of the immobilization and hybridization assays.

Molecule	Δf (Hz)	Δm ($\frac{ng}{cm^2}$)
DNA-c {2}, {3}	-1518 ± 415	255 ± 73
DNA-t {5}	-654 ± 182	115 ± 32
Streptavidin {6}	-1368 ± 284	241 ± 50

Table 3. Mass and frequency changes of the molecular coating assay.

Molecule	Δf (Hz)	Δm ($\frac{ng}{cm^2}$)
DNA-c {3}	-1234.53	218
DNA-c {4}	-406.97	71.74
DNA-t {7}	-877.13	155
DNA-t {8}	22.95	-4.04
Streptavidin {9}	-1746.32	308
Streptavidin {10}	-63.43	11

Table 4. Mass and frequency changes of the immobilization and hybridization assay in 100 MHz crystals.

Molecule	Δf (Hz)	Δm ($\frac{ng}{cm^2}$)
DNA-c (2)	-7319	309
DNA-c (3)	-1239	52.3
DNA-t (5)	-3816	161
Streptavidin (6)	-8529	349

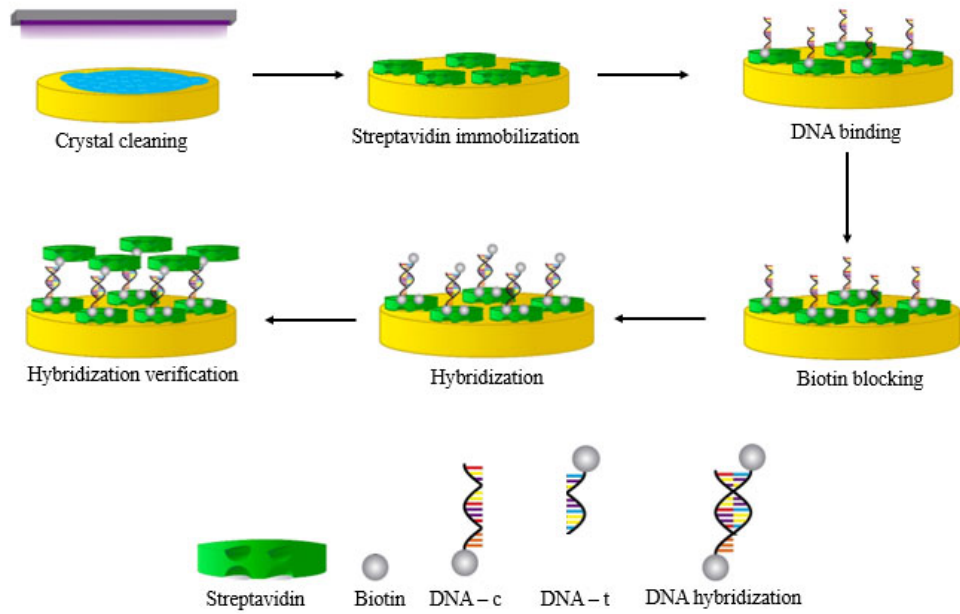


Figure 1. Diagram of the steps of immobilization and hybridization using the streptavidin-biotin binding methodology. DNA-c is the bioreceptor probe and DNA-t is the target probe.

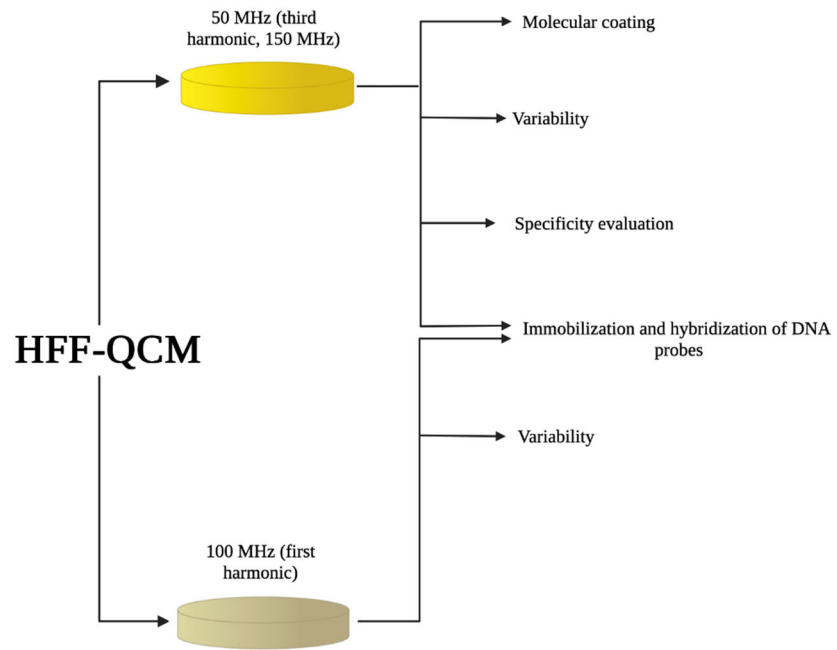


Figure 2. Tests performed on the crystals of fundamental frequencies of 50 and 100 MHz. The 50 MHz crystal was evaluated in the third harmonic (150 MHz)

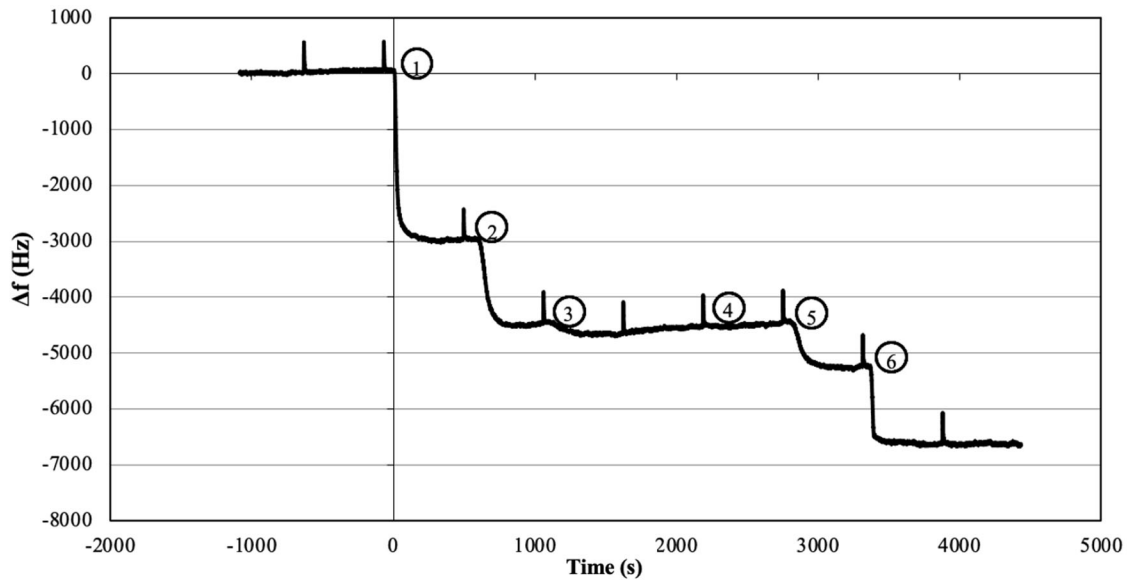


Figure 3. Immobilization and hybridization assay on a 50 MHz piezoelectric crystal in the third harmonic (150 MHz). The first step is the injection of streptavidin solution [50 $\mu\text{g}/\text{mL}$], the second and the third step corresponds to the immobilization of DNA probe (DNA-c) [1 μM], the fourth step is the injection of biotin solution [100 μM], the fifth step is the hybridization process with the DNA-t [1 μM], and finally, the sixth step is the addition of streptavidin [50 $\mu\text{g}/\text{mL}$].

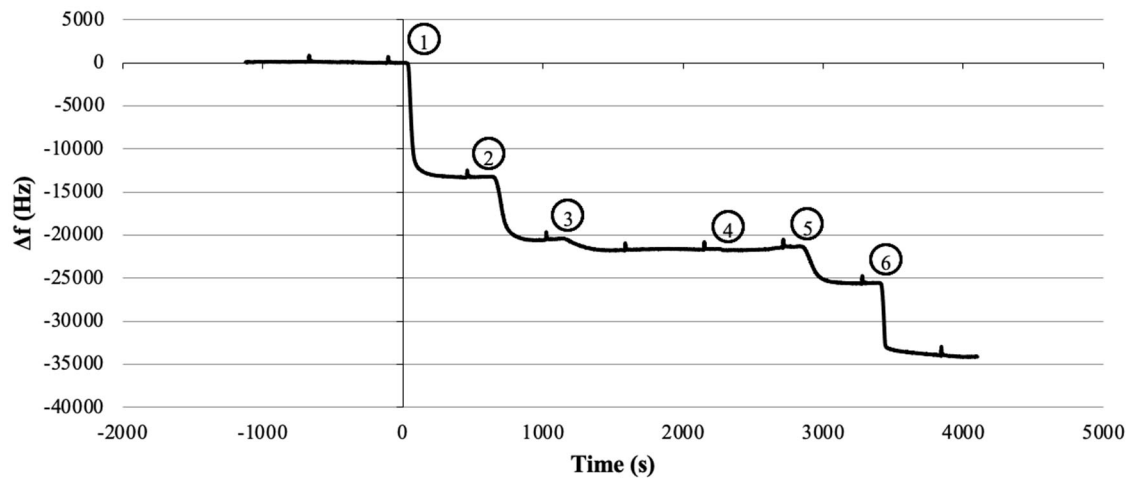


Figure 4. Immobilization and hybridization assay using the streptavidin-biotin methodology in a 100 MHz piezoelectric crystal. The first step is the injection of streptavidin solution [50 $\mu\text{g/mL}$], the second and the third step corresponds to the immobilization of DNA probe (DNA-c) [1 μM], the fourth step is the injection of biotin solution [100 μM], the fifth step is the hybridization process with the DNA-t [1 μM], and finally, the sixth step is the addition of streptavidin [50 $\mu\text{g/mL}$].

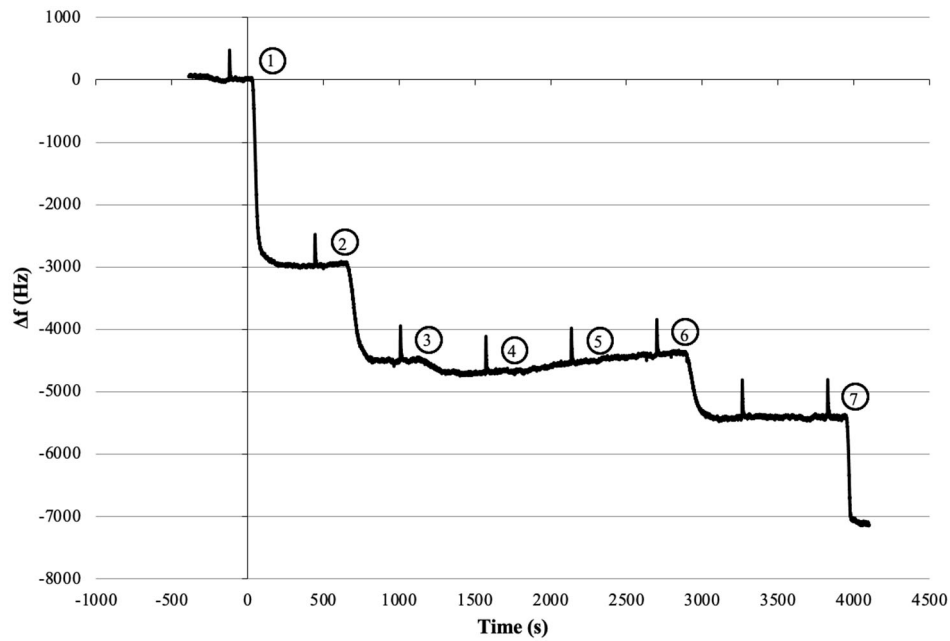


Figure 5. Hybridization control assay on a 50 MHz piezoelectric crystal in the third harmonic (150 MHz). The first step is the injection of the streptavidin solution [50 $\mu\text{g}/\text{mL}$], the second and the third steps represent the change in frequency associated with the immobilization of DNA-c [1 μM], the fourth step represents the biotin solution passed through the fluidic system [100 μM], the fifth step represents the control sequence [1 μM], the sixth step is the hybridization process with DNA-t [1 μM], and the seventh step represent the injection of streptavidin [50 $\mu\text{g}/\text{mL}$].